Enhanced Quadratic Programming via Pseudo-Transient Continuation: An Application to Model Predictive Control

Cognitive Raman Amplifier Control Using an Evolutionary Optimization Strategy

Giacomo Borraccini[(1)]*, Stefano Staullu[(2)], Stefano Piciaccia[(3)], Alberto Tanzi[(3)], Gabriele Galimberti[(3)], and Vittorio Curri[(1)]
[(1)] Politecnico di Torino, Turin, Italy; [(2)] LINKS Foundation, Turin, Italy; [(3)] Cisco Photonics, Vimercate, Italy
giacomo.borraccini@polito.it

***Abstract*—In this work, a cognitive Raman amplifier controller using an evolutionary optimization strategy for both in-field device calibration and optimal pump power configuration design is presented. The conceived methodology allows to jointly characterize the physical layer properties of the optical fiber span, such as the fiber attenuation profile, the entities of the lumped losses due to mechanical connectors or splices, the polarization coefficients between each Raman pump pair and the Raman efficiency curve. The developed framework expects to work using optical channel monitors (OCMs) as telemetry device and it has been experimentally validated, obtaining outstanding results in terms of precision on a C-band setup.**

***Index Terms*—Raman amplification, optical fiber networks, evolutionary optimization strategy.**

I. Introduction

THE increasing interest in Raman amplification and its consequent adoption within modern optical network infrastructures is justified by the multiple benefits that this technology provides to system performance in terms of maximum reach and operating rate [1]. As Raman amplification is nonlinear and distributed, the control of a Raman amplifier is challenging, since the pump power levels have to be set according to the target specifications and characteristics of the other devices that compose the system. Furthermore, there are some properties of the system which cannot be estimated with sufficient accuracy, such as the connector losses, the Raman efficiency curve and the pump state of polarization (SOP), which strongly affect the overall behaviour of the amplifier. Focusing on the SOP, a low Raman pump degree of polarization (DOP) allows a more suitable management of the optical line system, by reducing the impact of polarization-dependent phenomena [2]. The residual DOP of the pumps originates from the manufacturing process, giving an unexpected gain profile when completely depolarized pumps are assumed, as high power levels are involved that propagate in the same direction.

In previous works, the authors have already addressed the problem of the control of Raman amplifiers proposing a software-defined controller architecture [3] able to automatize the operation of the amplifier both in single- and multi-band transmission with a large set of gain target features [4]. An in-depth investigation has been carried out regarding the development of rapid and accurate probing procedures which allow the single amplifier to tailor its operation within the specific context in which it is inserted according to the available telemetry devices, such as optical channel monitors (OCMs) [5], [6] or standard photodiodes [7]. In this work, an original cognitive Raman amplifier controller is proposed adopting an evolutionary optimization strategy both to calibrate the device in field and to design the pump power configuration. In particular, after the installation of the apparatus, the first step is the determination of the set of physical layer parameters that allows the physical layer model to reproduce by emulation the experimental behaviour of the system. This characterization process aims to retrieve an equivalent model of the single fiber span modifying the values of the physical layer parameters by exploiting the comparison between the emulated output and the in-field measurements obtained in the same working point conditions. Once the physical layer parameters are extracted, the amplifier pumps have to be set to achieve the required gain target. The pump design process consists in emulating the behaviour of the system under different working point conditions changing the power levels of each pumps and in evaluating the relevant features of the emulated gain profile with respect to the targets. This study is focused on the determination of the optimal gain profile without considering the resulting amplified spontaneous emission (ASE) noise. The conceived approach represents an alternative effective solution to massive data-driven techniques [8] in automatizing Raman amplifiers and adapting the system after modifications of the scenario, such as fiber cut events.

II. Methodology

The software framework is based on the fiber span assumption reported in Fig. 1. It is composed by three elements which are an in-line amplifier (ILA), a series of fiber spools and a Raman card. Each ILA consists in an erbium-doped fiber amplifier (EDFA) equipped with OCMs at both terminals, a photodiode to measure the residual power of the counter-propagating Raman pumps and an optical time domain reflectometer (OTDR), to detect the position of mechanical

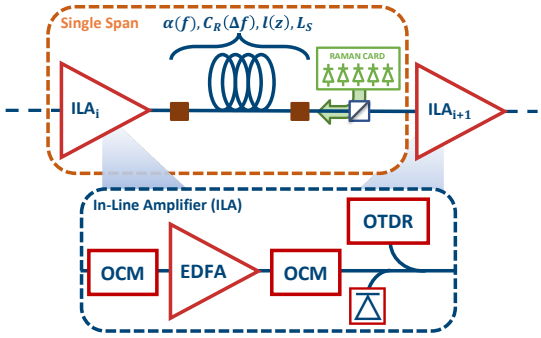

Fig. 1. Assumed optical fiber span scheme.

connectors. In this study, the fiber span is modelled by a set of physical layer parameters such as the total length, L_S, the entity and the position of the lumped losses along the span, $l(z)$, the loss coefficient function, $\alpha(f)$, and the Raman efficiency curve, $C_R(\Delta f)$. The Raman card is mounted in counter-propagating configuration by means of a circulator and it contains a set of laser pumps, each one characterized by a specific frequency, launch power level and polarization state.

The adopted physical layer model provides the numerical solution of the stimulated Raman scattering (SRS) system of differential equations [9] only for the counter-propagating pumps:

$$\frac{dP_i(z)}{dz} = P_i(z)\, l(z) \cdot \Bigg[-\alpha(f_i) + \\ + \sum_{j=i+1}^{N_P} k_{\mathrm{pol}}^{i,j}\, C_R^{i,j} P_j(z) - \sum_{j=1}^{i-1} \frac{f_j}{f_i}\, k_{\mathrm{pol}}^{i,j}\, C_R^{i,j} P_j(z) \Bigg], \tag{1}$$

where z is the discretized spatial axis which goes from 0 to L_S, N_P is the total number of pumps, $i, j = 1, 2, \ldots, N_P$ are the indices used to identify the specific pump, P_i is the power level at the frequency of the i-th pump, f_i, and at the position z. The polarization coefficient related to a specific couple of pumps, $k_{\mathrm{pol}}^{i,j}$, takes into account the polarization vector alignment between counter-propagating pumps [1]. It is a symmetrical matrix with null main diagonal where each element can be between 0 and 2 where the value 2 means that the couple of pumps has aligned polarization vectors, 1 if the pumps are completely depolarized and a low value close to 0 if the two polarization vectors are orthogonal. After the computation of the power spatial evolution of the pumps, the on-off gain is calculated using the analytical expression in undepleted pump condition:

$$\mathrm{G_{OO}}(f_n) = \exp\left(\sum_{i=1}^{N_P} \int_0^{L_S} C_R^{n,i} P_i(\zeta) d\zeta \right), \tag{2}$$

considering the overall gain on the specific forward-propagating channel as the sum of all the pump contributions, each one assumed as independent.

After the hardware installation, the developed methodology plans to execute two consecutive optimization steps to make the Raman amplifier operative: the physical layer characterization of the fiber span and the definition of the working point configuration of the amplifier. For both the steps, given the nonlinear nature of the physical layer model and the complexity of the problems, the optimization algorithm adopted in this study is the co-variance matrix adaptation evolutionary strategy (CMA-ES) [10]. The use of other optimization algorithms does not compromise the validity of the developed methodology. The choice is exclusively related to the characteristics of the achieved solution in terms of time and precision.

Step 1 *[Physical layer characterization]*: The aim of this optimization step is to retrieve the physical layer parameters which allow the model to match the experimental behaviour of the system under fixed working conditions.

The framework requires a specific set of measurements to get a complete overview of the system behavior. Firstly, the OTDR scans the fiber span detecting the position of all the lumped losses and the total length. Then, the total loss at the frequency of the Raman pumps is measured turning on each pump individually at the maximum power and reading the residual power at the other span terminal thanks to the photodiode. Finally, an arbitrary number of on-off gain profiles are measured defining the pump power configuration a-priori, turning on the EDFA in order to have a propagating ASE full-channel load and measuring the received spectrum through the OCM with the pumps turned on and off. The on-off gain is computed through the operative definition as the ratio between the propagating power spectra at the Raman amplifier side with the pumps respectively turned on and off. The shape of the produced ASE full-channel load is not significant, thanks to the use of OCMs. It is important to verify through the photodiode that the input ASE full-channel load power is low enough to do not affect the Raman pump power evolution, achieving the undepleted pump condition. The number of measured on-off gain profile has to be defined in order to probe different working regions of the system, appropriately choosing the pump configurations according to the delivered total power.

The set of physical layer parameters to optimize is the following: 1) loss coefficient function, $\alpha(f)$, 2) Raman efficiency, $C_R(\Delta f)$, 3) lumped losses, $l(z)$, 4) polarization coefficient matrix, k_{pol}. The loss coefficient function is described through a phenomenological model using four parameters that take into account the Rayleigh scattering, the infra-red absorption and the fiber water peak [11]. The Raman efficiency curve is parametrized using two parameters which describe the concentration of Germanium in the fiber, determining the shape of the normalized curve, and the absolute scale factor of the profile [12]. The total number of lumped losses depend on the result of the OTDR analysis. Given its definition, the number of parameters to optimize regarding the polarization coefficient matrix is equal to $\sum_{i=0}^{N_P-1} i$.

These parameters are jointly optimized emulating at each iteration all the on-off gain profiles obtained in the predefined pump power configurations feeding the physical layer model with a single extracted set of physical parameters. The goodness of the solution is tailored on the following objective function:

$$\min \sum_{j=1}^{N_{\mathrm{G}}} \sqrt{ \sum_{i=1}^{N_{\mathrm{SAMPLE}}} \left[\mathrm{G}_j^{\mathrm{MEAS}}(f_i) - \mathrm{G}_j^{\mathrm{EMU}}(f_i) \right]^2 }, \tag{3}$$

where N_{G} is the number of measured on-off gain profiles, N_{SAMPLE} is the number of evaluated points of the spectrum, $\mathrm{G}_j^{\mathrm{MEAS}}$ is the j-th measured profiles obtained using a specific pump power configuration and $\mathrm{G}_j^{\mathrm{EMU}}$ is the corresponding emulated profile. The optimal set of physical parameters has to allow to emulate with the lowest possible error the measured gain profiles according to the different pump configurations.

This formulation allows to fully characterize the Raman amplifier, probing its behaviour within the specific scenario and addressing the definition of the optimal set of physical layer

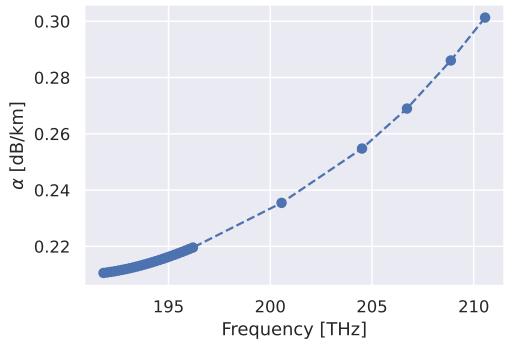

Fig. 2. Characterization results: loss coefficient function, $\alpha(f)$.

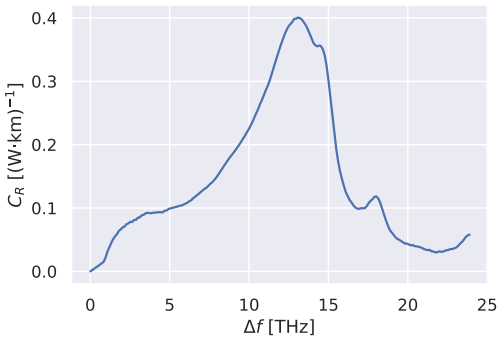

Fig. 3. Characterization results: Raman efficiency $C_R(\Delta f)$.

TABLE I
CHARACTERIZATION RESULTS: LUMPED LOSSES

$l(z=0)$ [dB]	$l(z=50.3\,\text{km})$ [dB]	$l(z=101.3\,\text{km}=L_S)$ [dB]
0.952	0.958	0.954

parameters on the direction of an equivalent representation of the system based on the given physical layer model.

***Step 2** [Working point configuration]*: Given a set of physical layer parameters, the second optimization step defines a pump power configuration that produces a gain profile which matches the design constraints in terms of mean gain and tilt.

Using the optimal set of parameters within the physical layer model, the variables to optimize are the launch power levels of each pump of the Raman card. The optimization algorithm extracts at each iteration a launch pump power configuration and evaluates the produced on-off gain profile using the model. The design process requires two constraints as input values which are the mean gain target, $\mathrm{G_{tar}}$, and the gain tilt target, $\mathrm{T_{tar}}$. The cost of the solution is evaluated on the base of the following objective function:

$$\min \quad \frac{1}{\mathrm{G_{tar}}} \cdot \left|\mathrm{G_{tar}} - \overline{\mathrm{G}}\right| + \left|\mathrm{T_{tar}} - \mathrm{T}\right| + \Delta\mathrm{G}, \qquad (4)$$

where, considering the emulated on-off gain profile $\mathrm{G_{OO}}(f_{ch})$, $\overline{\mathrm{G}}$ is the mean gain value, T is the angular coefficient of the linear regression and $\Delta\mathrm{G}$ is the gain ripple computed as the maximum distance with respect the linear regression. The function is built to achieve the design constraints annulling the first two terms and to minimize the dispersion of the profile with respect to its linear regression focusing on the gain ripple.

III. EXPERIMENTAL SETUP & RESULTS

The experimental laboratory setup used to reproduce the single span scheme depicted in Fig. 1 is composed by the following devices: a commercial ILA, working in ASE mode and filling the whole C-band with flat noise power; a couple of standard single mode fiber spools creating a span 100 km long (nominal length); a commercial Raman card composed by five independent counter-propagating optical pumps (Tab. III); an optical spectrum analyzer, in order to measure both the transmitted and received spectra.

Firstly, the results obtained during the physical layer characterization are reported. In particular, the derived loss coefficient function and Raman efficiency curve are depicted in Figs. 2 and 3, the OTDR analysis and the estimated lumped losses are shown in Tab. I, the extracted polarization matrix is reported in Tab. II. In order to obtain this set of physical layer parameters, three on-off gain profiles have been measured configuring the pumps at three different power regimes. Fig. 4 shows the comparison between the emulations performed with the optimal set of physical layer parameters and the measured on-off gain profiles obtained setting all the pumps respectively at the maximum values, 130 mW and 100 mW. This choice of the launch pump power configurations allows to satisfactorily inspect the dynamics of the Raman amplifier and to keep limited the optimization time, which increases with the number of on-off gain profiles to emulate. In the considered case, the physical layer characterization takes a variable time to finish the optimization which is of the order of the tens of minutes.

TABLE II
CHARACTERIZATION RESULTS: POLARIZATION COEFFICIENT MATRIX

	$\mathrm{P_1}$	$\mathrm{P_2}$	$\mathrm{P_3}$	$\mathrm{P_4}$	$\mathrm{P_5}$
$\mathrm{P_1}$	0	1.6481	1.3318	1.4736	0.8465
$\mathrm{P_2}$	1.6481	0	0.0005	0.0058	0.0156
$\mathrm{P_3}$	1.3318	0.0005	0	0.5724	0.01559
$\mathrm{P_4}$	1.4736	0.0058	0.5724	0	1.68794
$\mathrm{P_5}$	0.8465	0.0156	0.01559	1.68794	0

Then, in order to test the effectiveness of the methodology, the design process of the launch pump power configuration is run for all the couple of constraints derived by the combination of 10, 11, 12 dB as mean gain value and -0.2, 0, 0.2 dB/THz as tilt value. The optimization time of the design process using

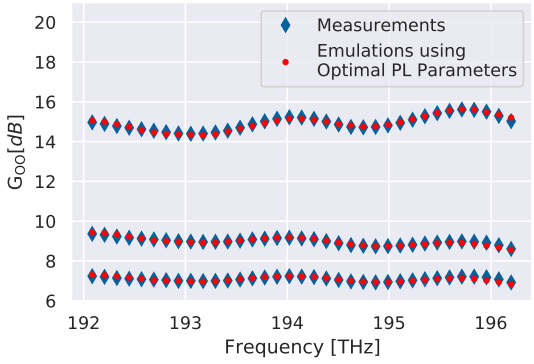

Fig. 4. Measured on-off gain profiles at three different power regimes: all the pumps at the relative maximum launch power level, 130 mW and 100 mW (blue diamonds); emulated gain profiles using the same pump configurations and the optimal set of physical layer parameters (red points).

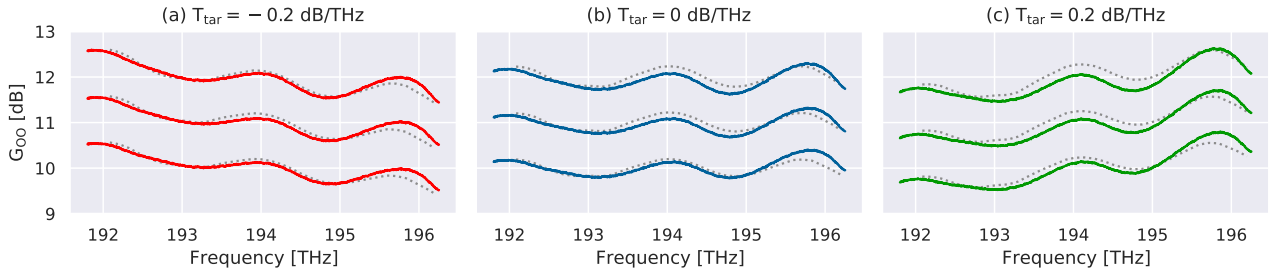

Fig. 5. Measured (solid line) and emulated (dot line) on-off gain profile for each designed pump power configuration.

TABLE III
DESIGNED PUMP POWER CONFIGURATIONS

Pump Number		#1	#2	#3	#4	#5
G_{tar} [dB]	T_{tar} [dB/THz]	Pump Power Levels [mW]				
10	-0.2	161.4	113.7	171.0	130.3	166.0
11	-0.2	179.6	105.3	198.2	145.7	202.3
12	-0.2	180.0	130.0	200.0	171.7	228.8
10	0	176.0	64.3	176.0	150.3	199.2
11	0	151.9	98.3	186.0	161.3	220.9
12	0	152.0	112.4	200.0	180.9	248.5
10	0.2	179.9	20.4	180.6	168.2	230.7
11	0.2	156.6	53.8	191.0	178.1	253.6
12	0.2	138.8	86.5	198.3	192.9	273.5
		Pump Maximum Power Levels [mW]				
		180.0	130.0	200.0	320.0	360.0
		Pump Frequencies [THz]				
		200.6	204.5	206.7	208.9	210.6

TABLE IV
RESULT ANALYSIS

G_{tar} [dB]	T_{tar} [dB/THz]	$\overline{G}$ [dB]	T [dB/THz]	ΔG [dB]	RMSE [dB]	E_{MAX} [dB]
10	-0.2	10.0	-0.159	0.5	0.09	0.24
11	-0.2	11.0	-0.155	0.6	0.10	0.25
12	-0.2	11.9	-0.166	0.6	0.08	0.20
10	0	10.0	0.045	0.6	0.10	0.27
11	0	10.9	0.0214	0.7	0.10	0.16
12	0	11.9	0.012	0.7	0.11	0.18
10	0.2	10.0	0.258	0.7	0.12	0.28
11	0.2	10.9	0.234	0.7	0.14	0.22
12	0.2	11.9	0.205	0.7	0.16	0.27

five Raman pumps is less than one minute for all the evaluated configurations. Tab. III contains all the designed pump power configurations for each couple of given constraints, reporting the maximum power value and frequency of each pump. The complete set of measured and emulated on-off gain profile is depicted in Fig. 5 and the relative summary of some aggregated metrics is reported in Tab. IV. Observing the experimental results, the designed Raman pump power configurations correctly produce the required mean gain, presenting a slight positive tilt offset with respect to the targets. The values of ripples are limited below 0.7 dB, showing a satisfactory degree of flatness around the linear regression of the profile. Comparing the predicted and the measured profiles, the maximum absolute error, E_{MAX}, is on average 0.23 dB. Regarding the root-mean-square error, RMSE, the discrepancy between the profiles increases when a positive tilt is required, since the Raman pumps at high frequencies deliver an higher amount of power. In this condition, the interaction between pumps is more intense and the effective on-off gain profile is more affected by the uncertainty related to the deduced physical layer parameters.

IV. CONCLUSION

In this work, a methodology based on an optimization approach to control a Raman amplifier within a fiber span is presented, making its operation cognitive and autonomous. The framework has been experimentally validated in laboratory on a single C-band fiber span using an evolutionary optimization strategy. The achieved on-off gain profiles show an excellent match with respect to the predictions for all the designed pump power configurations.

REFERENCES

[1] J. Bromage, "Raman amplification for fiber communications systems," *journal of lightwave technology*, vol. 22, no. 1, p. 79, 2004.
[2] Q. Lin and G. P. Agrawal, "Vector theory of stimulated raman scattering and its application to fiber-based raman amplifiers," *JOSA B*, vol. 20, no. 8, pp. 1616–1631, 2003.
[3] G. Borraccini, A. Ferrari, S. Straullu, A. Nespola, A. D'Amico, S. Piciaccia, G. Galimberti, A. Tanzi, S. Turolla, and V. Curri, "Softwarized and autonomous raman amplifiers in multi-band open optical networks," in *2020 International Conference on Optical Network Design and Modeling (ONDM)*. IEEE, 2020, pp. 1–6.
[4] G. Borraccini, S. Straullu, A. Ferrari, S. Piciaccia, G. Galimberti, and V. Curri, "Flexible and autonomous multi-band raman amplifiers," in *2020 IEEE Photonics Conference (IPC)*. IEEE, 2020, pp. 1–2.
[5] G. Borraccini, S. Staullu, A. Ferrari, S. Piciaccia, G. Galimberti, A. Tanzi, and V. Curri, "Autonomous raman amplifiers in software-defined optical transport networks," in *GLOBECOM 2020-2020 IEEE Global Communications Conference*. IEEE, 2020, pp. 1–6.
[6] G. Borraccini, S. Straullu, A. D'Amico, A. Nespola, S. Piciaccia, A. Tanzi, G. Galimberti, and V. Curri, "Autonomous raman amplifiers in multi-band software-defined optical transport networks," *Journal of Optical Communications and Networking*, vol. 13, no. 10, pp. E53–E62, 2021.
[7] G. Borraccini, S. Staullu, S. Piciaccia, A. Tanzi, A. Nespola, G. Galimberti, and V. Curri, "Autonomous raman amplifiers using standard integrated network equipment," *IEEE Photonics Technology Letters*, 2021.
[8] U. C. De Moura, M. A. Iqbal, M. Kamalian, L. Krzczanowicz, F. Da Ros, A. M. R. Brusin, A. Carena, W. Forysiak, S. Turitsyn, and D. Zibar, "Multi–band programmable gain raman amplifier," *Journal of Lightwave Technology*, vol. 39, no. 2, pp. 429–438, 2020.
[9] S. Tariq and J. C. Palais, "A computer model of non-dispersion-limited stimulated raman scattering in optical fiber multiple-channel communications," *Journal of lightwave technology*, vol. 11, no. 12, pp. 1914–1924, 1993.
[10] N. Hansen, Y. Akimoto, and P. Baudis, "CMA-ES/pycma on Github," Zenodo, DOI:10.5281/zenodo.2559634, Feb. 2019. [Online]. Available: https://doi.org/10.5281/zenodo.2559634
[11] G. Borraccini, A. D'Amico, S. Straullu, A. Nespola, S. Piciaccia, A. Tanzi, G. Galimberti, S. Bottacchi, S. Swail, and V. Curri, "Cognitive and autonomous qot-driven optical line controller," *Journal of Optical Communications and Networking*, vol. 13, no. 10, pp. E23–E31, 2021.
[12] K. Rottwitt, J. Bromage, A. J. Stentz, L. Leng, M. E. Lines, and H. Smith, "Scaling of the raman gain coefficient: applications to germanosilicate fibers," *Journal of lightwave technology*, vol. 21, no. 7, p. 1652, 2003.